Supplementary for "Helicity and Polarization Gradient Optical Trapping in Evanescent Fields"

Jinsheng Lu,[1] Vincent Ginis,[1,2] Soon Wei Daniel Lim,[1] and Federico Capasso[1,*]

[1] *Harvard John A. Paulson School of Engineering and Applied Sciences, 9 Oxford Street, Cambridge, Massachusetts 02138, USA*

[2] *Data Lab and Applied Physics, Vrije Universiteit Brussel, 1050 Brussel, Belgium*

(Dated: August 10, 2023)

CONTENTS

* capasso@seas.harvard.edu

S1. NUMERICAL SIMULATIONS

We perform the full-wave 3D electromagnetic simulations using Ansys Lumerical FDTD to obtain the total electric and magnetic fields ($\mathbf{E}^{tot}$ and $\mathbf{H}^{tot}$), including the incident fields and the scattering fields. The optical forces for the silicon nanoparticle in the total-internal-reflection (TIR) system and the microsphere near the microfiber are numerically evaluated using the Maxwell stress tensor, which is defined as [1]

$$T_{ij}=\varepsilon E_i^{tot*}E_j^{tot}+\mu H_i^{tot*}H_j^{tot}-\frac{1}{2}\delta_{ij}(\varepsilon|\mathbf{E}^{tot}|^2+\mu|\mathbf{H}^{tot}|^2) \tag{S1}$$

where ε and μ are the permittivity and permeability of the environment, respectively. δ_{ij} is the Kronecker delta. The time-averaged optical forces are obtained by integrating the tensor on a closed surface surrounding the nanoparticle or microparticle.

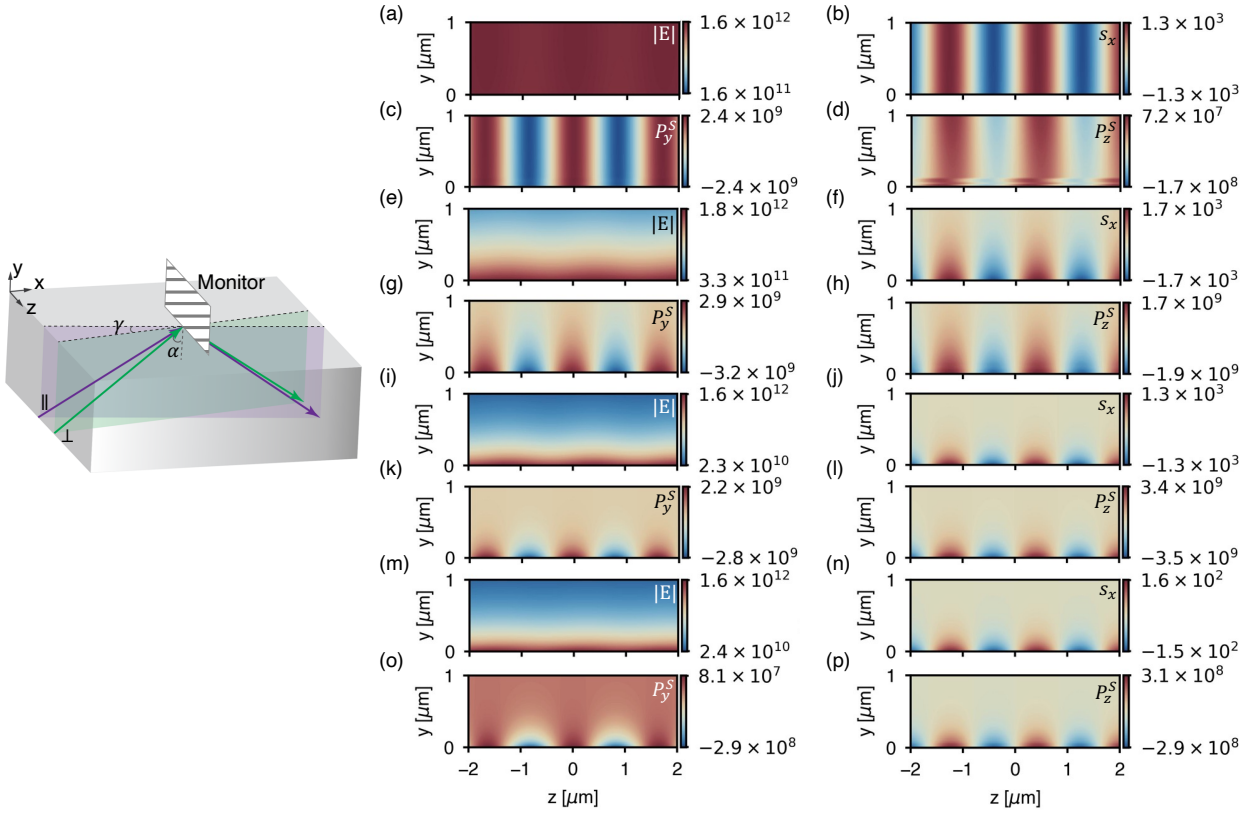

FIG. S1. Electric fields and optical momenta in a TIR system at different incident angles. Electric field amplitude |E| (a),(e),(i),(m), longitudinal spin angular momentum density s_x (b),(f),(j),(n), transverse Belinfante spin momentum P_z^S (d),(h),(l),(p), vertical Belinfante spin momentum P_y^S (c),(g),(k),(o) distributions in the transverse plane when the incident angle at the water-glass interface α is 61 (a-d), 62 (e-h), and 65 (i-p) deg and when the two beams in the TIR system are with orthogonal linear polarizations (a-l) and orthogonal circular polarizations (m-p). $\gamma = 20$ deg. The wavelength of the incident light is 785 nm. The intensity of the incident light is 1 mW/μm^2 per beam. The unit of the electric amplitude, SAM density, and BSM density are V/m, kg/(m $\cdot$ s), and kg/(m^2 $\cdot$ s), respectively.

S2. LATERAL OPTICAL FORCE AND BELINFANTE SPIN MOMENTUM

Optical forces on a particle come from the momentum transfer from light to the particle. The electromagnetic field momentum $\mathbf{P}$ is defined as $\mathbf{P} = \mathrm{Re}(\mathbf{E}^* \times \mathbf{H})/2$, which can be divided into canonical momentum $\mathbf{P}^{\mathrm{O}}$ and the Belinfante spin momentum $\mathbf{P}^{\mathrm{S}}$: $\mathbf{P} = \mathbf{P}^{\mathrm{O}} + \mathbf{P}^{\mathrm{S}}$. The canonical momentum is defined as [2]

$$\begin{aligned} \mathbf{P}^{\mathrm{O}} = \mathbf{P}_{\mathrm{e}}^{\mathrm{O}} + \mathbf{P}_{\mathrm{m}}^{\mathrm{O}} &= \frac{c^2}{4\omega}\mathrm{Im}\left(\epsilon\mathbf{E}^* \cdot (\nabla)\mathbf{E} + \mu\mathbf{H}^* \cdot (\nabla)\mathbf{H}\right) \\ \mathbf{P}_{\mathrm{e}}^{\mathrm{O}} &= \frac{c^2\epsilon}{4\omega}\mathrm{Im}\left(\mathbf{E}^* \cdot (\nabla)\mathbf{E}\right) \\ \mathbf{P}_{\mathrm{m}}^{\mathrm{O}} &= \frac{c^2\mu}{4\omega}\mathrm{Im}\left(\mathbf{H}^* \cdot (\nabla)\mathbf{H}\right) \end{aligned} \tag{S2}$$

The Belinfante spin momentum is defined as [2]

$$\begin{aligned} \mathbf{P}^{\mathrm{S}} &= \frac{1}{2}\nabla \times \mathbf{s} = \mathbf{P}_{\mathrm{e}}^{\mathrm{S}} + \mathbf{P}_{\mathrm{m}}^{\mathrm{S}} \\ \mathbf{P}_{\mathrm{e}}^{\mathrm{S}} &= \frac{c^2\epsilon}{8\omega}\nabla \times \mathrm{Im}\left(\mathbf{E}^* \times \mathbf{E}\right) \\ \mathbf{P}_{\mathrm{m}}^{\mathrm{S}} &= \frac{c^2\mu}{8\omega}\nabla \times \mathrm{Im}\left(\mathbf{H}^* \times \mathbf{H}\right) \end{aligned} \tag{S3}$$

where the spin angular momentum $\mathbf{s}$ is defined as

$$\mathbf{s} = \frac{c^2}{4\omega}\mathrm{Im}\left(\epsilon\mathbf{E}^* \times \mathbf{E} + \mu\mathbf{H}^* \times \mathbf{H}\right) \tag{S4}$$

In an evanescent field of the TIR system (light propagates along the x direction), the Belinfante spin momentum can be simplified as [2]

$$\mathbf{P}^{\mathrm{S}} = \frac{1}{2}\nabla_z s_x \mathbf{e}_y - \frac{1}{2}\nabla_y s_x \mathbf{e}_z \tag{S5}$$

where $\mathbf{e}_y$ and $\mathbf{e}_z$ are the unit vectors. The Belinfante spin momentum has two components in the evanescent field of the TIR system: the transverse component P_z^S and the vertical component P_y^S, which can introduce helicity-dependent forces to a small probe particle in the transverse direction ($F_z^S \propto P_z^S = -\frac{1}{2}\nabla_y s_x$) and in the vertical direction ($F_y^S \propto P_y^S = \frac{1}{2}\nabla_z s_x$).

In the transverse direction, the optical force comes from the transverse Belinfante spin momentum, called the lateral optical force (F_z^S). Even though there is still a small field intensity variation in the transverse direction which can introduce a gradient force (F_z^g), the intensity gradient in the transverse direction is very small. Therefore, the corresponding gradient force is negligible compared with the lateral optical force ($F_z^g \ll F_z^S$, see Fig. S2).

S3. ANALYTICAL CALCULATIONS OF OPTICAL FORCES ON DIPOLE PARTICLES

When the size of a particle is far smaller than the wavelength, we can treat the particle as a dipole, and the optical force on a dipole particle can be decomposed into three terms: the force comes from the electric-induced dipole ($\mathbf{F_p}$), the force comes from magnetic-induced dipole ($\mathbf{F_m}$), and the force comes from the dipole-dipole higher-order interaction between the induced electric and magnetic moments ($\mathbf{F_{pm}}$). These three terms can be further expressed as (please refer to the detailed derivation process in Eqs. (13)-(17) in Aleksandr Y. Bekshaev's paper [3, 4])

$$\begin{aligned}\mathbf{F} &= \mathbf{F_p} + \mathbf{F_m} + \mathbf{F_{pm}} \\ &= \nabla U + 2\omega\mu \operatorname{Im}[\alpha_{\mathrm{e}}]\, \mathbf{P}_{\mathrm{e}}^{\mathrm{O}} + 2\omega\epsilon \operatorname{Im}[\alpha_{\mathrm{m}}]\, \mathbf{P}_{\mathrm{m}}^{\mathrm{O}} - \frac{ck^4}{12\pi}\left(2\operatorname{Re}[\alpha_e\alpha_m^*]\left(\mathbf{P}^{\mathrm{O}} + \mathbf{P}^{\mathrm{S}}\right) - \operatorname{Im}[\alpha_e\alpha_m^*]\operatorname{Im}[\mathbf{E}\times\mathbf{H}^*]\right)\end{aligned} \tag{S6}$$

where $U = \frac{1}{4}\left(\operatorname{Re}[\alpha_{\mathrm{e}}]\,|\mathbf{E}|^2 + \operatorname{Re}[\alpha_{\mathrm{m}}]\,|\mathbf{H}|^2\right)$ is the free energy of the field. $\mathbf{E}$ and $\mathbf{H}$ are the incident electric and magnetic fields interacting with the dipole particle. α_e and α_m are the electric and magnetic polarizabilities of the particle, which can be expressed in terms of the Mie coefficients a_1 and b_1 as follows: $\alpha_e = \frac{i6\pi\epsilon}{k^3}a_1$ and $\alpha_m = \frac{i6\pi\mu}{k^3}b_1$. k is the wavevector. ϵ and μ are the permittivity and permeability of the environment, respectively. c is the speed of light in a vacuum. $\mathbf{P}^{\mathrm{O}}$ is the canonical momentum density which includes the electric part $\mathbf{P}_{\mathrm{m}}^{\mathrm{O}}$ and the magnetic part $\mathbf{P}_{\mathrm{e}}^{\mathrm{O}}$.

These force terms, green in Eq. S6, coming from the electric-induced dipole or the magnetic-induced dipole, contain the gradient force (related to the gradient of field energy ∇U) and the scattering force (related to the canonical momentum $\mathbf{P}^{\mathrm{O}}$). The helicity-dependent force related to the Belinfante spin momentum ($\mathbf{P}^{\mathrm{S}}$) only exists in the violet-colored force term in Eq. S6 due to the higher-order interaction between the electric-induced dipole and the magnetic-induced dipoles, which also verified by the multipole decomposition results of a silicon particle at Mie resonances (Fig. S4).

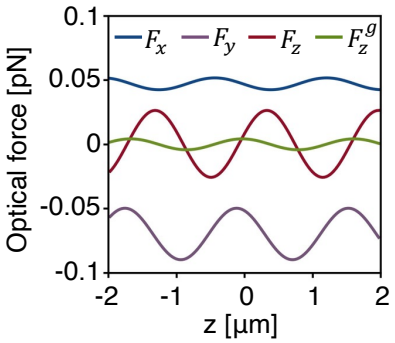

FIG. S2. Calculated optical forces of a Polystyrene particle with a diameter of 200 nm when varying the particle's position along the transverse direction in the TIR system when the incident two beams are with orthogonal linear polarizations. Blue curve: scattering force in the longitudinal direction (the x direction). Red curve: lateral optical force. Purple curve: total force in the vertical direction, including the intensity gradient force and the Belinfante spin momentum-induced helicity-dependent force. Green curve: the intensity gradient force in the transverse direction. $n_{\mathrm{glass}} = 1.52$, $n_{\mathrm{water}} = 1.33$, $\gamma = 20$ deg, and $\alpha = 65$ deg (which is larger than the critical angle $\alpha_c = 61$ deg). The working wavelength is 785 nm. The intensity of the incident light is 1 mW/μm^2 per beam.

S4. REPULSIVE FORCE IN EVANESCENT FIELDS

In the vertical direction of the TIR system, a well-known helicity-independent conservative gradient force exists due to the intensity decay in the evanescent field (F_y^g). This force generally functions as an attractive force to pull the particle close to the interface ($F_y^g < 0$). Besides, the vertical Belinfante spin momentum contributes a helicity-dependent nonconservative optical force (F_y^S) which can be comparable to the gradient force in the vertical direction. The total optical force in the vertical direction can be expressed as

$$F_y = F_y^g + F_y^S \tag{S7}$$

According to Eq. S6, the above equation can be further written as

$$F_y = \nabla_y U - \kappa P_y^S \tag{S8}$$

where $\kappa = \frac{ck^4}{6\pi} \mathrm{Re}\left[\alpha_e \alpha_m^*\right]$ is a coefficient relating the force and the Belinfante spin momentum for a dipole particle.

The helicity-dependent force can enhance ($F_y^S < 0$), counteract ($F_y^S = -|F_y^g|$), or reverse ($F_y^S > |F_y^g|$) the gradient force in the vertical direction [Fig. S3(b,f,j)].

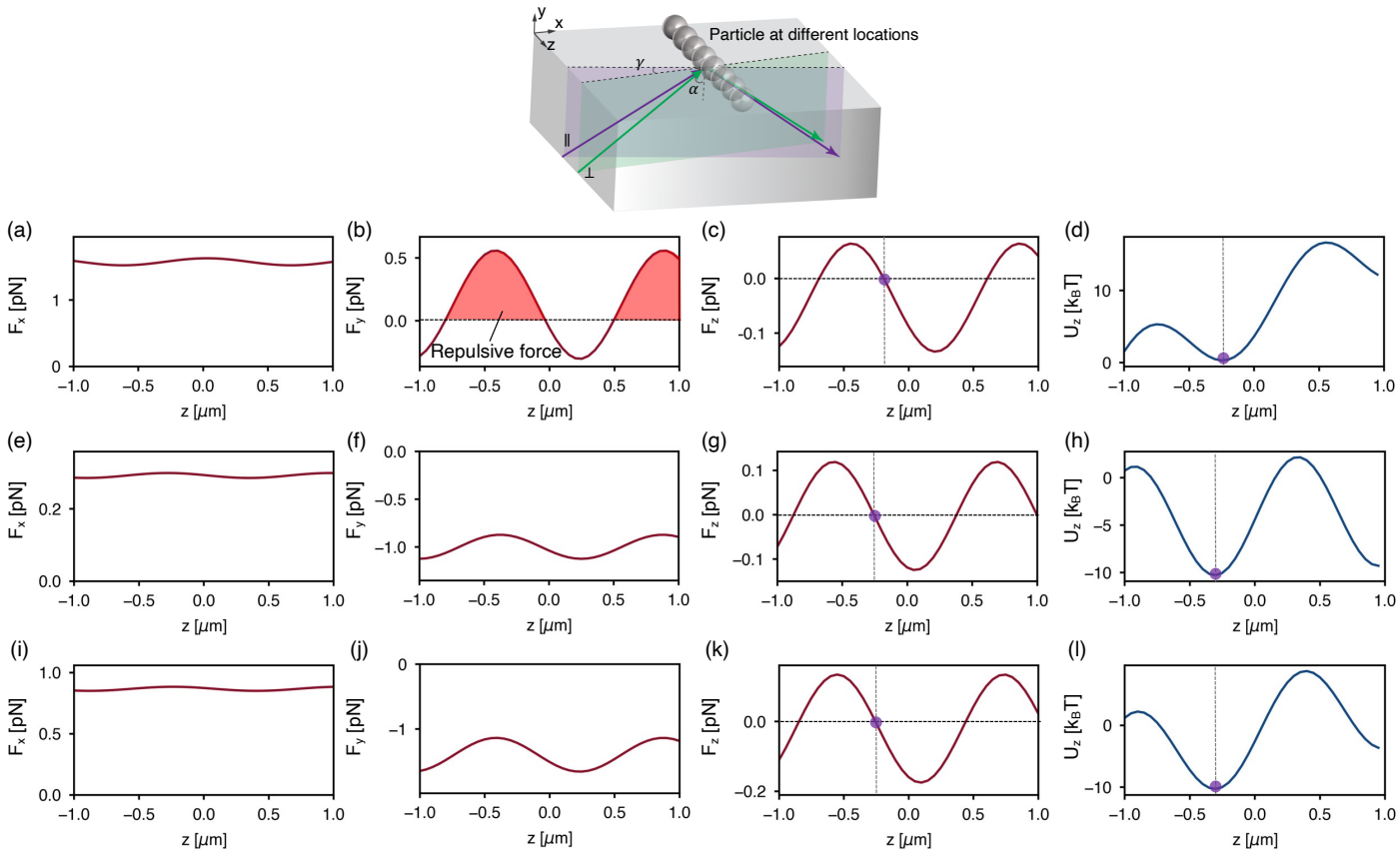

FIG. S3. Calculated optical forces and helicity gradient optical trapping potentials of a Polystyrene particle with a diameter of 500 nm when varying the particle's position along the transverse direction in the TIR system when the incident two beams have orthogonal linear polarizations. The angle α of the incident beams in the TIR system is 61 (a-d), 62 (e-h), and 65 (i-l) deg. The red region in (b) indicates that the particle experience a repulsive (positive) force in the vertical direction in the evanescent field. The purple dots in (c), (d), (g), (h), (k), and (l) represent the trapping positions of the particle in the transverse direction. $n_{\mathrm{glass}} = 1.52$, $n_{\mathrm{water}} = 1.33$, $\gamma = 20$ deg, and $\alpha = 65$ deg. The wavelength of the incident light is 600 nm. The intensity of the incident light is 1 mW/μm^2 per beam.

S5. MULTIPOLE DECOMPOSITION OF MIE-RESONANCE PARTICLES

Here we perform the multipole analysis of the scattering cross section for the Mie resonance particles. We only consider the electric dipole and the magnetic dipole because the silicon particle in our system is small (diameter: 200 nm). Higher-order multiples should be considered when the particle size is large. The multipoles can be obtained from the total field inside the silicon nanoparticle according to the equations [5]

$$\begin{aligned} \mathbf{p} &= \epsilon_0 \left(\epsilon_r - 1\right) \int \mathbf{E}(\mathbf{r}) dV \\ \mathbf{m} &= \frac{i\omega\epsilon_0 \left(\epsilon_r - 1\right)}{2} \int \left(\mathbf{r} \times \mathbf{E}(\mathbf{r})\right) dV \end{aligned} \tag{S9}$$

where ϵ_0 and ϵ_r are the vacuum permittivity and relative permittivity of the silicon nanoparticle, respectively. $\mathbf{p}$ and $\mathbf{m}$ are the electric and magnetic dipole moments induced in the silicon nanoparticle. The total scattering cross section can be expressed as

$$\begin{aligned} \sigma_{sca} &= \sigma_{sca}^{\mathbf{p}} + \sigma_{sca}^{\mathbf{m}} + ... \\ &\approx \frac{c^2 k_0^4 Z_0}{12\pi I_0} |\mathbf{p}|^2 + \frac{k_0^4 Z_0}{12\pi I_0} |\mathbf{m}|^2 \end{aligned} \tag{S10}$$

where c is the speed of light. k_0 is the wave number. Z_0 is the vacuum wave impedance. I_0 is the light intensity.

The calculated total scattering cross section of a silicon nanoparticle with a diameter of 200 nm using the multipole analysis is consistent with the simulated scattering cross section, as shown in Fig. S4. The silicon nanoparticle supports both the electric dipole and magnetic dipole resonances. The dipole-dipole interaction induces a lateral optical force on the silicon nanoparticle.

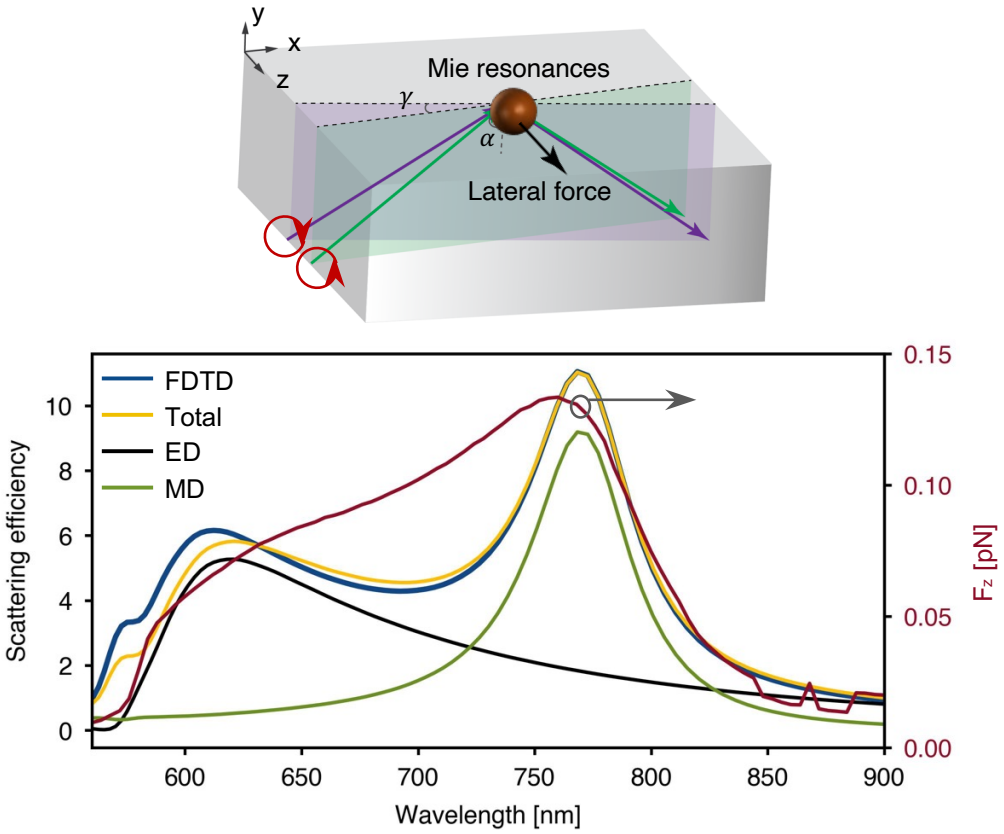

FIG. S4. Simulated scattering spectra (blue line), calculated multipole decompositions (total contributions, yellow line; electric dipole (ED), black line; magnetic dipole (MD), green line), and the lateral optical force (red line) of a silicon nanoparticle with a diameter of 200 nm. The scattering spectra of the silicon nanoparticle are simulated and calculated when the silicon particle is in the free space illuminated by a plane wave. The lateral optical force curve is obtained from Fig. 2(c) in the main text when the particle is placed in the TIR system ($z = 0.4\ \mu m$), and incident beams have orthogonal circular polarizations.

S6. RESONANCE-INDUCED PHASE SHIFT EFFECT

The resonances of silicon nanoparticles introduce a phase shift to the helicity standing wave in the transverse direction of the TIR system, resulting in the particle not necessarily being trapped at a position where helicity changes from positive to negative, as shown in Fig. S5(a). This phase shift effect comes from the polarization-dependent resonance

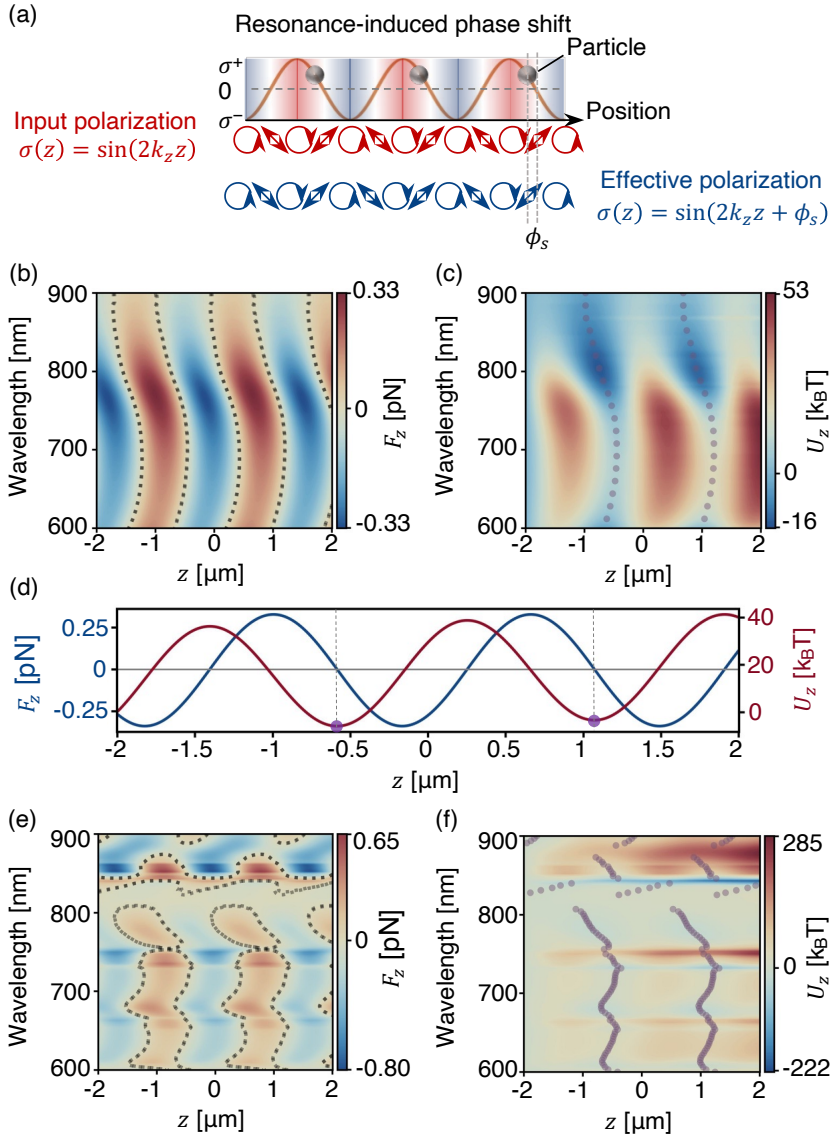

FIG. S5. Phase shift effect of the helicity gradient optical trapping of a Mie-resonance particle when the two beams in the TIR system have orthogonal linear polarizations. (a) Schematics show the effective polarization distribution when there exist a phase shift ϕ_s due to the Mie-resonance. (b),(c) Calculated spectra of the lateral optical force (b) and trapping potential (c) of a silicon nanoparticle with a diameter of 200 nm in the TIR system. The two beams have orthogonal linear polarizations. The black dashed lines in (b) indicate where the lateral force is zero ($F_z = 0$). The purple dots in (c) indicate the trapping positions. (d) Calculated lateral optical force and trapping potential at the resonance wavelength of 768 nm, obtained from (b) and (c). (e),(f) Calculated spectra of the lateral optical force (e) and trapping potential (f) of a silicon nanoparticle with a diameter of 500 nm in the TIR system. In simulations, $n_{\text{glass}} = 1.52$, $n_{\text{water}} = 1.33$, $\gamma = 20$ deg, and $\alpha = 65$ deg. The intensity of the incident light is 1 mW/μm^2 per beam.

of the nanoparticle in the evanescent field of the TIR system. More specifically, the nanoparticle is at resonance when the input beam has transverse electric (TE) polarization but not when the input beam has transverse magnetic (TM) polarization. Note that the resonance generates a phase shift. This polarization-dependent resonance results in a phase difference of ϕ_s to the TE and TM polarized beams. Therefore, when the two beams have orthogonal linear polarization in the TIR system, the polarization-dependent resonance of the silicon nanoparticle experiences an effective polarization distribution in the transverse (z) direction, which can be described by the Jones vector $\mathbf{J}_{\text{eff}}(z)$.

$$\mathbf{J}_{\text{eff}}(z) = \frac{1}{\sqrt{2}} \begin{pmatrix} e^{-ik_z z} \\ e^{ik_z z} e^{i\phi_s} \end{pmatrix} \tag{S11}$$

where k_z is the wave number in the transverse direction. ϕ_s is the polarization-dependent phase shift between the TE and TM polarizations in the near field at resonances.

The corresponding effective helicity distribution in the transverse direction is:

$$\sigma_{\text{eff}}(z) = \sin(2k_z z + \phi_s) \tag{S12}$$

We calculate the lateral optical force of a silicon nanoparticle with a diameter of 200 nm in the TIR system when the polarization of input beams are orthogonal linear polarizations, as shown in Fig. S5(b). The corresponding trapping potential in the transverse direction is shown in Fig. S5(c). Since the resonance phase shift is wavelength dependent, the trapping positions (represented by the purple dots) of the silicon nanoparticle shift with the wavelength of the input beams. The lateral optical force and trapping potential reach 0.33 pN and 47.1 k_BT at the resonant peak wavelength of 768 nm, respectively [Fig. S5(d)]. We also calculate the lateral optical force of a silicon nanoparticle with a diameter of 500 nm under the same conditions, as shown in Figs. S5(e) and S5(f). The larger the silicon nanoparticle, the more resonances it supports, showing a clearer and more complex phase shift effect.

S7. THE INFLUENCE OF THE MISALIGNMENT OF TWO BEAMS IN THE TIR SYSTEM

In this section, we investigate the influence of the misalignment of the two beams (cross angle, incident angle, and polarization angle) in the TIR system (Fig. 1 in the main text) on the performance of the helicity gradient optical trapping. This system can still work well when the two beams are slightly misaligned. Furthermore, the polarizations of the two beams do not need to be exactly orthogonal. The helicity gradient optical trapping performance in the TIR system is robust with respect to these experimental imperfections.

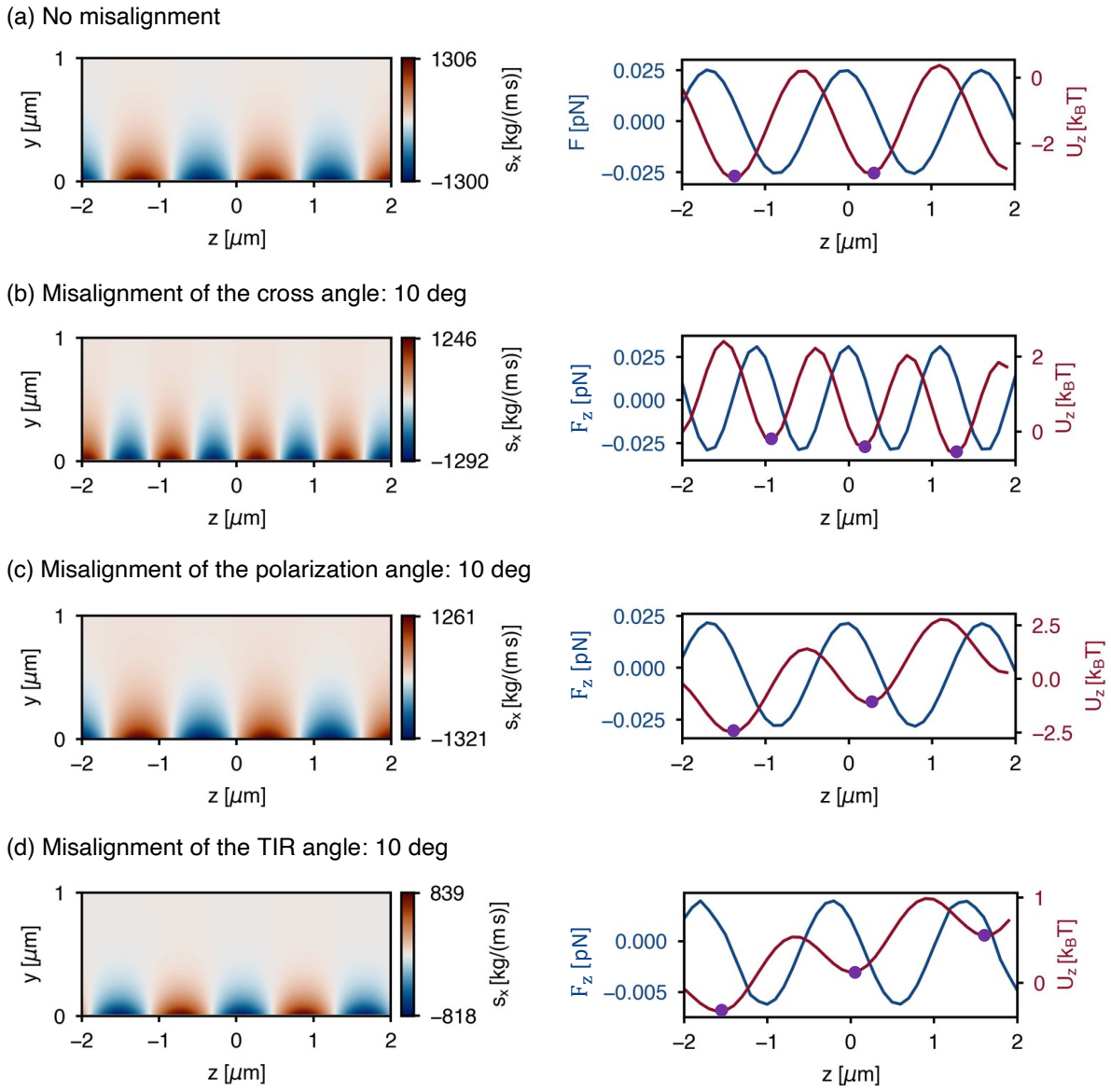

FIG. S6. The influence of the misalignment of the two beams in Fig.1 of the main text. (a-d) Calculated Spin volume density sx (left panel) and optical lateral force Fz and trapping potential Uz (right panel) when the two beams are without misalignment (a), with a misalignment of the cross angle of the two beams by 10 deg (b), with a misalignment of the polarization angle by 10 deg (c), with a misalignment of the total internal reflection angle by 10 deg (d). The purple dots indicate the trapping sites. The cross angle γ becomes 30 deg due to misalignment in (b). The polarization angles of the two beams in (c) are 0 deg and 100 deg. Note that the polarization angles of the TE and TM polarized beam are 0 deg and 90 deg, respectively. The incident angles of the two beams are $\alpha_1 = 65$ deg and $\alpha_2 = 75$ deg, respectively. The other parameters used in simulations here are the same as Fig. 1 in the main text.

When the two beams are aligned exactly and with orthogonal polarizations, the spin volume density, optical lateral force, and trapping potential are shown in Fig. S6(a). The period of the helicity (spin) variation in the transverse direction (the z direction) is about 1.8 μm. We consider three possible sources of experimental error. Firstly, let us consider a misalignment of the cross angle of the two beams by 10 deg (Fig. S6(b)). This results in the cross angle of the two beams increasing to 30 deg. The period of the helicity variation is reduced to 1.2 μm. The trapping potential well becomes slightly asymmetric. However, the optical lateral force's amplitude and trapping potential depth remains almost the same, retaining good trapping ability. Secondly, when the polarization of the two beams is misaligned (by a polarization angle of 10 deg) so that they are no longer orthogonal, the results are shown in Fig. S6(c). Due to a

more asymmetric potential well, though the amplitude of the optical lateral force decreases slightly, and the trapping potential depth is reduced to about 80% of that without misalignment. This is still good enough for trapping. Thirdly, when the incident angle of the two beams is misaligned by 10 deg, the results show that both the amplitude of the optical force and the trapping potential depth (0.8 k_BT) are reduced by around five times compared to that without misalignment (Fig. S6(d)). Helicity gradient optical trapping in this system is still feasible. On the one hand, we can increase the input laser intensity from 1 mW/μm^2 to 12.5 mW/μm^2. Then the trapping potential depth will be increased from 0.8 k_BT to 10 k_BT, ensuring stable optical trapping (a potential depth of 10 k_BT is usually defined as a trapping threshold). On the other hand, we can also use a particle with a larger size or higher refractive index to enhance the optical force and trapping potential depth.

[1] L. Novotny and B. Hecht, *Principles of Nano-Optics* (Cambridge university press, 2012).

[2] K. Y. Bliokh, A. Y. Bekshaev, and F. Nori, Extraordinary momentum and spin in evanescent waves, Nat. Commun. **5**, 3300 (2014).

[3] A. Y. Bekshaev, Subwavelength particles in an inhomogeneous light field: optical forces associated with the spin and orbital energy flows, J. Opt. **15**, 044004 (2013).

[4] A. Y. Bekshaev, Corrigendum: Subwavelength particles in an inhomogeneous light field: optical forces associated with the spin and orbital energy flows (2013 j. opt. 15 044004), J. Opt. **18**, 029501 (2016).

[5] D. Sikdar, W. Cheng, and M. Premaratne, Optically resonant magneto-electric cubic nanoantennas for ultra-directional light scattering, J. Appl. Phys. **117**, 083101 (2015).